Colloid Polym Sci (2015) 293:913–923
DOI 10.1007/s00396-014-3478-3

ORIGINAL CONTRIBUTION

Synthesis and micellization properties of triblock copolymers PDMAEMA-*b*-PCL-*b*-PDMAEMA and their applications in the fabrication of amphotericin B-loaded nanocontainers

Ivonne L. Diaz · Leon D. Perez

Received: 13 September 2014 / Revised: 23 November 2014 / Accepted: 28 November 2014 / Published online: 12 December 2014

Abstract In this study, we report the synthesis of PDMAEMA-*b*-PCL-*b*-PDMAEMA via ATRP starting from two dibromide-end polycaprolactone (PCL) of 2 and 10 kDa. The copolymerization was confirmed by nuclear magnetic resonance and gel permeation chromatography. The micellar properties of copolymers with different compositions were studied at pH 5.0, 6.0, 7.0, and 7.5. According to results, properties such as critical micellar concentration (CMC), hydrophobicity of micelle cores, and particle size strongly depend on the length of PCL. The pH shows an important effect on the size of the colloidal aggregates. Micelles obtained from copolymers with the lowest polymerization degree of both segments showed to be more appropriate for the encapsulation of amphotericin B (AmB).

Keywords Polycaprolactone · Block copolymer · Micelles · Atom transference radical polymerization

Introduction

The use of polymer micelles (PM) obtained by self-assembly of block copolymers in aqueous media, as nanocontainers for hydrophobic or poorly soluble drugs have devoted great interest [1–3]. PMs are composed of two separated domains, an inner core and an outer shell. The outer shell controls the micelle solubility and in vivo interaction with tissues and cells, while the inner core is responsible for drug loading and stability. The properties of PM result from their high colloidal stability which is afforded by the presence of hydrophilic segments, and their low critical micellar concentration (CMC) compared with low molecular weight surfactants. Some of the advantages of using PMs as drug nanocarriers include their ability to protect the drugs allowing them to maintain their activity, reduce their toxicity and secondary effects during the circulation time, and also permit controlling its concentration in the plasma [4, 5].

Although there is a huge number of block copolymers with potential biomedical applications, amphiphilic block copolymers composed of polycaprolactone (PCL) and poly(*N*,*N*-dimethylaminoethyl methacrylate) (PDMAEMA) evoke great interest due to the outstanding physical and chemical properties of the individual blocks. PCL, a hydrophobic polymer approved by the FDA for biomedical applications, is biocompatible, biodegradable, and highly permeable to drugs and presents high capacity of encapsulating hydrophobic substances [6, 7]. There are numerous reports concerning about the synthesis of block copolymers containing PCL with application in the fabrication of micelles for drug delivery. PCL is commonly combined with hydrophilic blocks such as polyvynilpyrrolidone, polyethyleneglycol (PEG), and poly(*N*-isopropylacrylamide) [8–11].

Although previous reports indicate that the elevated concentration of amino groups in the chains of PDMAEMA results in high toxicity, the copolymerization with polymers such as PCL and PEG not only reduces the concentration of amino groups but also imparts biocompability [12–15]. The biocompatibility of PDMAEMA achieved on its copolymerization summed to its pH responsive behavior render the materials containing it very promising for the design of sensitive drug delivery systems [16–20].

Atom transfer radical polymerization (ATRP) is a "controlled/living" radical polymerization widely used for its good control over molecular weight and dispersity and its applicability in the synthesis of polymers starting from preformed materials and surfaces [21, 22]. In this study, we started from

I. L. Diaz
Departamento de Química, Pontificia Universidad Javeriana, Carrera 7 No. 40-62, Bogotá, DC, Colombia

L. D. Perez (✉)
Departamento de Química, Universidad Nacional de Colombia, Carrera 45 No. 26-85, edificio 451 of 449, Bogotá, DC, Colombia
e-mail: ldperezp@unal.edu.co

two dibromide-end PCL samples having different molecular weight, 2 and 10 kDa. The triblock copolymer were obtained by the polymerization of 2-(dimethylamino)ethyl methacrylate (DMAEMA) using Cu(I)Br/*N*,*N*,*N*′,*N*″,*N*″-pentamethyldiethylenetriamine as catalyst and in the presence of Br-PCL-Br macroinitiators.

Although researches recently show that polymer materials containing segments of PCL and PDMAEMA can be potentially used in drug delivery applications [13, 15, 23–28], there is not a general consensus about the effect of their structure on their performance. The aim of this study is to establish relationships between the composition and molecular weight of triblock copolymers PDMAEMA-*b*-PCL-*b*-PDMAEMA with the colloidal properties of micelles obtained from their assembly in aqueous medium. This research also intends to determine the effect of properties of the PM such as CMC, core hydrophobicity, and size on their ability of encapsulating amphotericin B (AmB), which is an antifungal agent with excellent performance but poor solubility and toxicity that limit its pharmaceutical application [29]. Compared with conventional drugs, AmB has high molecular weight, exhibits amphiphilic character, and has high tendency to aggregate, which also determines its encapsulation in micellar aggregates.

Experimental part

Materials

DMAEMA (98 %) was passed through a column packed with basic alumina. α,ω-Dihydroxy-poly(ε-caprolactone) of M_n= 2 and 10 kDa was purified by precipitation from a mixture of tetrahydrofuran (THF) and methanol. 2-Bromoisobutyryl bromide (BIBB; 98 %), triethylamine (>99 %), cupper(I) bromide (CuBr; 98 %), *N*,*N*,*N*′,*N*″,*N*″-pentamethyldiethylenetriamine (PMDETA; 99 %), pyrene (98 %), anisole, and amphotericin B were used without any additional purification. All the reagents as well the solvents (hexane, dimethylsulfoxide, *N*,*N*-dimethylformamide, acetone, methanol, and tetrahydrofurane) were supplied by Sigma-Aldrich.

Synthesis procedures

Synthesis of Br-PCL-Br terminated In a typical procedure for PCL M_n=10 kDa, 5 g of diol-ended PCL (0.35 mmol) was dissolved in 50 mL of anhydrus dichloromethane with 500 μL of tryelthylamine (3.5 mmol) while stirring under argon atmosphere. After that, 431 μL of BIBB (3.5 mmol) is added dropwise to the abovementioned solution, previously cooled using an ice–water bath. The reaction mixture was stirred during 24 h at room temperature. The product was precipitated by the addition of an excess of methanol, recovered by filtration, and subjected to three precipitation cycles. The same procedure was used to modify PCL of 2 kDa.

Synthesis of PDMAEMA-b-PCL-b-PDMAEMA A typical protocol for ATRP of PDMAEMA using Br-PCL-Br (M_n= 10 kDa) as macroinitiator and Cu(I)Br/PMDETA was as follows: In a Schlenk tube, Br-PCL-Br (0.5 g, 36 μmol) was dissolved in 5 mL of anisole to which DMAEMA (0.61 g, 3.9 mmol) and PMDETA (12.5 mg, 72 μmol) were added. The system was purged with argon during 15 min and deoxygenated by three freeze–pump–thaw cycles. Then CuBr (5.2 mg, 36 μmol) was added, the system was degassed by two additional freeze–pump–thaw cycles, and the polymerization reaction was allowed to proceed at 60 °C, under argon atmosphere. The reaction product was passed through a column packed with basic alumina to eliminate cupper residuals and purified by three successive precipitations from a THF solution by the addition of either methanol or hexane depending on the composition of the copolymers.

Formation of micelle aggregates

The copolymer micelles were prepared by a nanoprecipitation method [30]. In detail, 20 mg copolymer sample was dissolved in 2.5 mL of acetone. Then, the solution was added dropwise into 5 mL of a buffer solution of pH 5.0, 6.0, 7.0, or 7.5 under vigorous stirring. The resulting dispersion was maintained under stirring during 24 h at room temperature to allow the acetone evaporation.

Characterization techniques

^{1}H NMR and ^{13}C NMR spectra were collected in a Bruker Avance III spectrometer operated at 300 MHz. Samples were dissolved in $CDCl_3$ and the spectra were recorded at 303 K. Chemical shifts (δ) were expressed in parts per million with respect to the $CDCl_3$ signals.

Molecular weight and distribution were measured by gel permeation chromatography (GPC) in a Waters HPLC equipped with a differential refraction index detector. The analyses were performed in THF at a flow rate of 0.8 mL/min using a HR 4E column. The calibration curve was constructed with standards of polystyrene with M_p values of 1920, 3250, 10,250, 24,000, 32,500, and 67,500 Da.

Micelles average diameter was determined by dynamic light scattering (DLS) using a Horiba LB 550 equipment using a detector located at 173°. The measurements were carried out at 23 °C in aqueous dilutions of the samples (≈1/20) prepared using deionized water (~18 MΩ cm), in order to avoid particle–particle interactions and multiple scattering effects, each dispersion

plot corresponds to an average of 128 measurements acquired during 2 s. ζ potential was measured using a zeta potential analyzer Malvern Zetasizer Nano ZS. ζ potential was determined three times for each sample.

For TEM analysis, 2 μL of the diluted samples (0.1 mg/mL) was spilled into a copper grid Formvar® coated and dried at room temperature during 24 h; the images were obtained in a Jeol 1400 plus microscope.

CMC of block copolymers was determined by fluorescence using pyrene as a fluorescence probe, based on procedures previously reported [31, 32]. Briefly, PDMAEMA-*b*-PCL-*b*-PDMAEMA micelles were prepared with various concentrations (3.8 to 8×10^{-6} mg/mL) with a fixed concentration of pyrene of 0.6 μM. The pH of the micelle dilutions were fixed at 5.0, 6.0, 7.0, and 7.5. Excitation spectra of pyrene from 300 to 360 nm were monitored at 390 nm for each dilution using a fluoresce spectrometer Cary Eclipse. The CMC was determined plotting the ratio of the intensities at 335 and 332 nm (I_{335}/I_{332}) vs log concentration.

Preparation of AmB-loaded micelles

A typical protocol for the preparation of AmB-loaded block copolymer micelles was as follows: 2 mg of AmB was dissolved in 2 mL of methanol and slowly droplet (10 μL/min) into 10 mL of a micelle solution at pH 5.0 containing 4 mg/mL of the corresponding copolymer. The resulting solution was gently stirred during 1 h under reduce pressure to eliminate methanol residuals. Finally, the dispersion was centrifuged at 10,000 rpm to eliminate the non-encapsulated AmB and lyophilized for its posterior use.

The amount of AmB encapsulated in the PMs was determined by UV–vis spectroscopy using a Varian Cary 100. The quantification was performed as follows, aliquots of 1 mL of encapsulated AmB aqueous dispersions were mixed with an equal volume of DMF and analyzed by UV–vis, and the quantification was performed using a calibration curved obtained from the absorbance at 411 nm, prepared by direct dilution of AmB in a 50:50 (vol/vol) water/DMF mixture.

The loading efficiency (DLE%) as well as the drug content (DLC%) were estimated using equations proposed by Zhang et al. [13] as follows:

$$\mathrm{DLC\%} = \frac{\text{amount of AmB in PMs}}{\text{amount of AmB} + \text{PMs}} \quad (1)$$

$$\mathrm{DLE\%} = \frac{\text{amount of AmB in PMs}}{\text{amount of AmB used for PMs preparation}} \quad (2)$$

Results and discussion

Synthesis of triblock copolymers PDMAEMA-*b*-PCL-*b*-PDMAEMA

Amphiphilic triblock copolymers PDMAEMA-*b*-PCL-*b*-PDMAEMA were synthesized by ATRP using a dibromide-end polycaprolactone (Br-PCL-Br) as macroinitiator and CuBr/PMDETA as a catalyst, as shown in Scheme 1.

Two α,ω-dihydroxy-PCL samples with different M_n values of 2 and 10 kDa were transformed into Br-PCL-Br by reacting with an excess of BIBB. The reaction was assessed by ^{1}H NMR; the anchorage of bromoisobutiryl groups was indicated by the absence of the signal at 3.62 ppm of the hydroxymethylene terminal groups of PCL, and also by the presence of a new signal at 1.96 ppm due to methyl groups of BIBB, as shown in Fig. 1.

Triblock copolymers PDMAEMA-*b*-PCL-*b*-PDMAEMA containing different lengths of PCL and PDMAEMA were synthesized using the reagent molar ratios and reaction times listed in Table 1. The block copolymerization was confirmed by NMR and GPC. A representative spectrum of a purified triblock copolymer PDMAEM-*b*-PCL-*b*-PDMAEMA is shown in Fig. 2a. The spectrum presents the characteristic signal of methylene (–CH_2–) groups in PCL (δ ~1.40, 1.67, 2.32, and 4.08 ppm) and also signals due to PDMAEMA block such as –CH_2–C(CO)–CH_3 (δ ~1.05 ppm), –CH_2–C–CH_3 (δ ~1.89), –N(CH_3)$_2$ (δ ~2.32 ppm), –CH_2–N(CH_3)$_2$ (δ ~2.61 ppm), and –O–CH_2–CH_2–N (δ ~4.08 ppm) are clearly distinguished [33, 34].

The average number molecular weight of the copolymers (M_n), and the polymerization degree of DMAEMA (X_{DMAEMA}) relative to PCL were estimated from the ^{1}H NMR, using equations showed below:

$$X_{\mathrm{DMAEMA}} = I_f \times \frac{M_n\mathrm{PCL}}{114} \quad (3)$$

$$M_n = M_n\mathrm{PCL} + (157.2 \times X_{\mathrm{DMAEMA}}) \quad (4)$$

Where I_f is the ratio of the intensity of signals at 2.61 ppm that corresponds to –CH_2–N groups of PDMAEMA, and 1.40 ppm assigned to –CH_2– of PCL.

^{13}C-APTNMR spectra were collected to further confirm the formation of block copolymers. As shown in Fig. 2b, the spectrum of P10D2 shows signals due to both segments; the presence of PCL segments is inferred by signals due to –CH_2– (δ ~24.74, 25.65, 28.48, 34.09, 64.25 ppm) and C=O (δ ~173.72 ppm). Whereas the segment of PDMAEMA is identified by resonance peaks such as –CH_2–C–CH_3 (δ ~44.77 ppm), –N(CH_3)$_2$ (δ ~45.45 ppm), –CH_2–C(CO)–CH_3 (δ ~55.17 ppm), –CH_2–N(CH_3)$_2$ (δ ~57.08 ppm), –O–

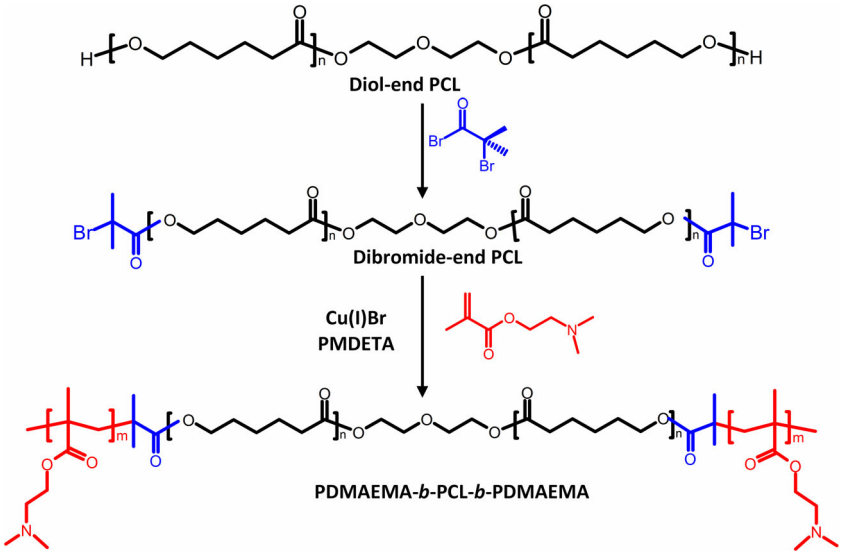

Scheme 1 Synthetic pathway of PDMAEMA-*b*-PCL-*b*-PDMAEMA triblock copolymers via ATRP of DMAEMA

CH_2–CH_2–N (δ ~63 ppm) and C=O (δ ~177 ppm). The assignation of signals was performed according to a previously published work [33].

GPC traces of block copolymers obtained at two different reaction times (Fig. 3a, b), show that the samples exhibit a monomodal distribution and also indicate that as the reaction proceeds, the hydrodynamic volume of the molecules increases. The molecular weight dispersities (*Đ*) obtained from a relative calibration curve made with PS standards are listed in Table 1. These values, typical of living free radical polymerizations, point out that under the selected conditions, there was control on the polymerization reactions. Further evidence of the controlled characteristics of the polymerization reactions using both macroinitiators is deduced from the linear dependence of $\ln[M_0]/[M]$ with time (Fig. 3c, d), which characterizes a first-order kinetics.

Self-assembly behavior of triblock copolymers

We first investigate the effect of the structure of triblock copolymers on their CMC in aqueous medium at pH 5. CMC besides serving as a strong evidence of the self-association of block copolymers, it is also an important parameter to evaluate the stability of micelles. Amphiphilic block copolymers with high CMC values seem to be unsuitable because the formed micelles may be dissociated after being administered into the body because of the dilution effect. From this point of view, a low CMC value is necessary for an efficient carrier.

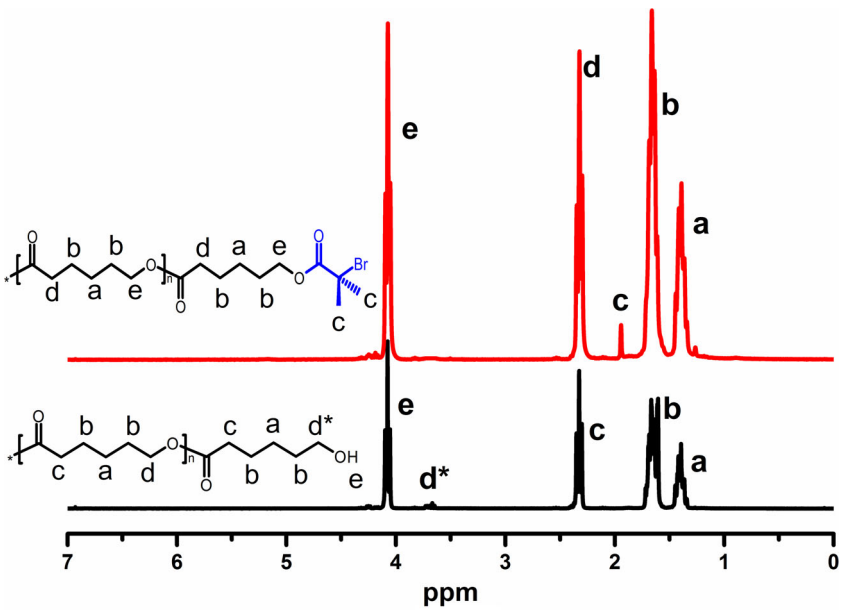

Fig. 1 ^{1}H NMR spectra of PCL and Br-PCL-Br in solution using $CDCl_3$ as a solvent

Table 1 Polymerization conditions and characterization of triblock copolymers PDMAEMA-*b*-PCL-*b*-PDMAEMA

Sample	Composition in the feed[a]	Reaction time (h)	Average composition	M_n[b] (kDa)	M_w/M_n[c]
PCL-2				2	1.04
P2D1	1:40:1:2	21	$DMAEMA_{11}$-*b*-CL_{17}-*b*-$DMAEMA_{11}$	5.4	1.39
P2D2	1:108:1:2	1	$DMAEMA_{19}$-*b*-CL_{17}-*b*-$DMAEMA_{19}$	7.9	1.09
P2D3	1:108:1:2	6	$DMAEMA_{28}$-*b*-CL_{17}-*b*-$DMAEMA_{28}$	10.7	1.40
PCL-10				10	1.09
P10D1	1:108:1:2	1	$DMAEMA_{28}$-*b*-CL_{88}-*b*-$DMAEMA_{28}$	18.8	1.17
P10D2	1:108:1:2	12	$DMAEMA_{39}$-*b*-CL_{88}-*b*-$DMAEMA_{39}$	22.3	1.09
P10D3	1:215:1:2	21	$DMAEMA_{61}$-*b*-CL_{88}-*b*-$DMAEMA_{61}$	29.2	1.15

[a] Reagents molar ratio Br-PCL-Br/DMAEMA/CuBr/PMDETA

[b] Estimated using ^{1}H NMR

[c] Estimated from GPC

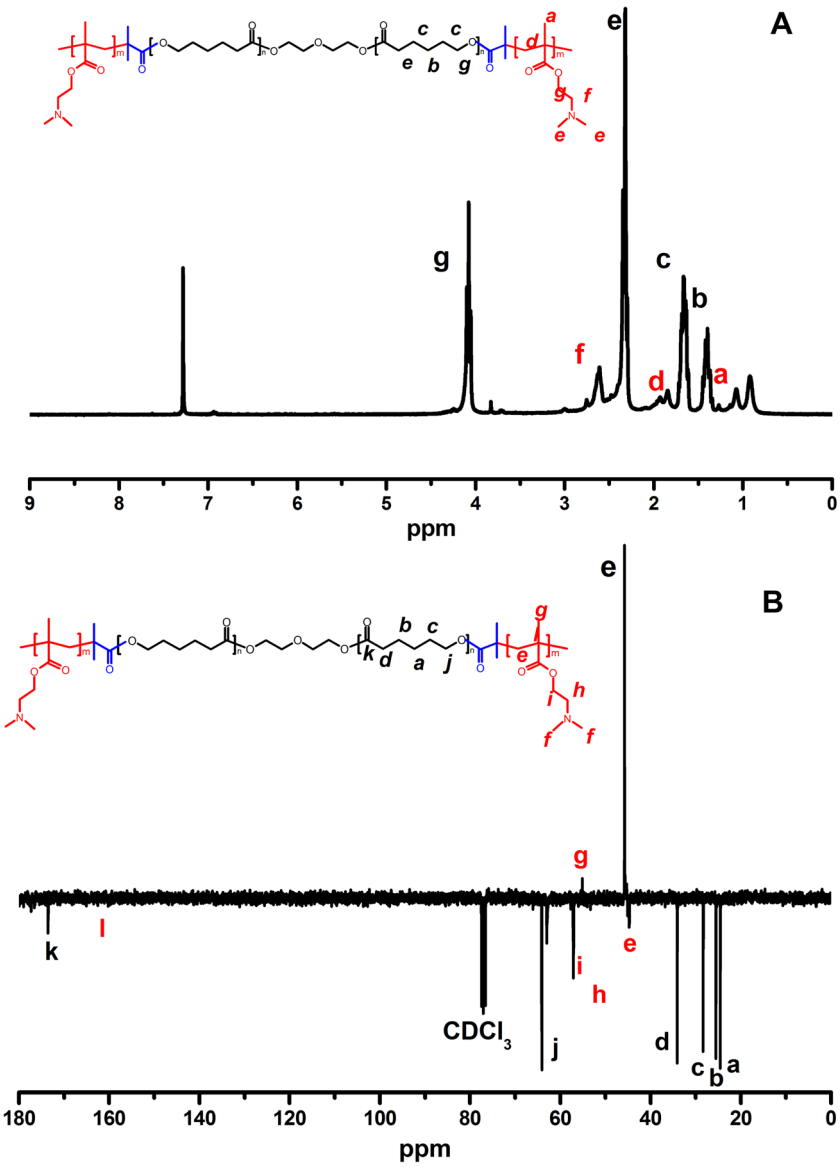

Fig. 2 Representative spectrum of triblock copolymer P10D2. **a** ^{1}H NMR and **b** ^{13}C-APT NMR

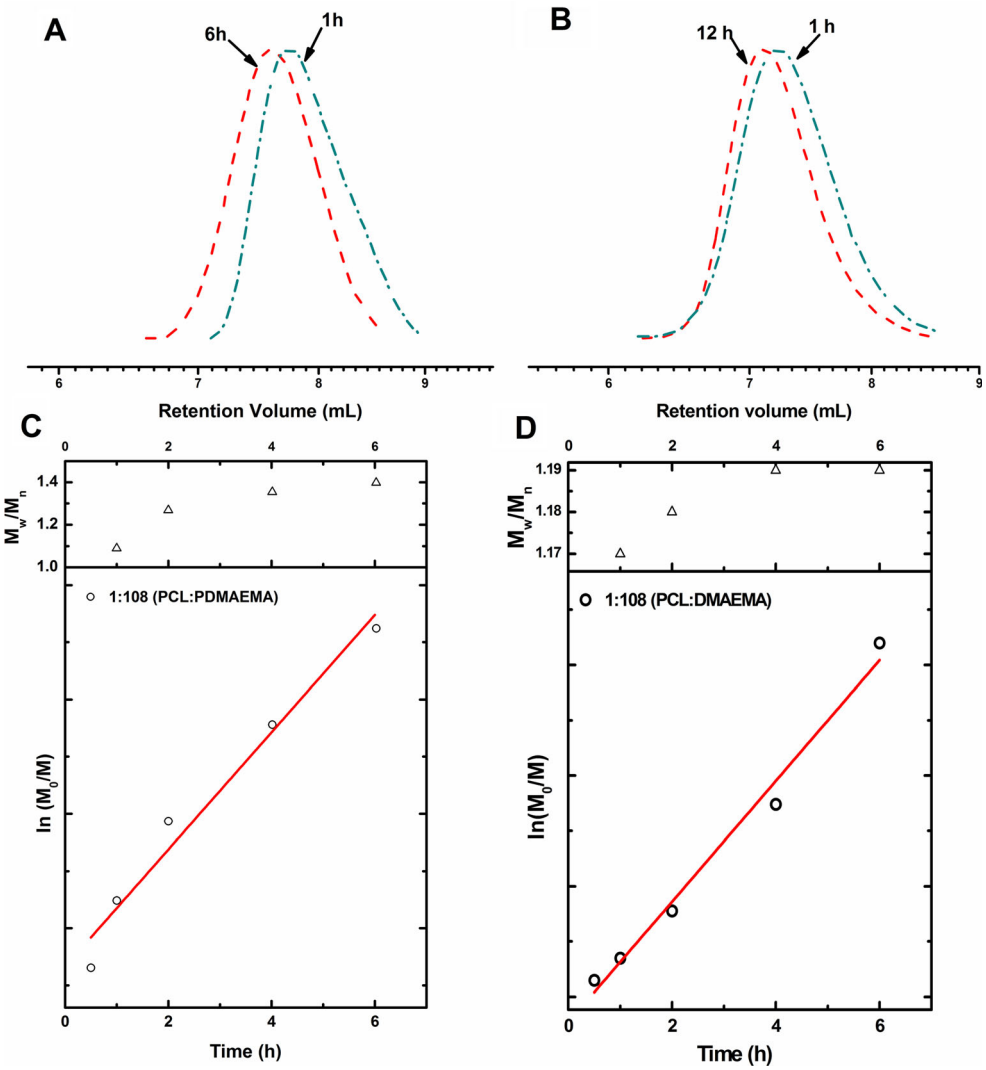

Fig. 3 GPC traces of PDMAEMA-*b*-PCL-*b*-PDMAEMA obtained from PCL **a** 2 and **b** 10 kDa at two different reaction times. Kinetic plots for the polymerization of DMAEMA using Br-PCL-Br of **c** 2 and **d** 10 kDa as macroinitiator

In this study, micelle formation was monitored by fluorometry using pyrene as a fluorescent probe. Pyrene strongly fluoresces in a non-polar environment, while in a polar environment it shows weak fluorescence intensity. This technique has been widely used to determine CMC for block copolymers and low molecular weight surfactants [13, 35]. Figure 4a shows the excitation spectra of pyrene monitored at 390 nm with different concentrations of copolymer P2D2. The strong dependence of the emission intensity of pyrene on the concentration of the block copolymer provides evidence of its aggregation and indicates that pyrene offers enough sensitivity for determining CMC [36]. From Fig. 4a, it is also observed that the maximum located at 332 nm (I_1) suffers at red shift to 335 nm (I_3) when the concentration of the copolymer increases.

Figure 4b shows the intensity ratio of I_{335}/I_{332} of pyrene excitation spectra as a function of the logarithm of copolymer concentration for P2D2 sample. The plot of I_{335}/I_{332} vs log C presents a sigmoid curve. For each copolymer, in the low concentration range, the ratio of I_{335}/I_{332} was almost constant. As the concentration of the copolymer increased, the signal intensity ratio exhibited a substantial increase reflecting the incorporation of pyrene into the hydrophobic domains. Thus, the CMC values were determined from the cross-over point in the low concentration range in Fig. 4b, and the results are listed in Table 2. Copolymers containing a PCL block of 2 kDa present CMC values in the range of 5.9 and 7.4, while in the case of copolymers with a PCL block of 10 kDa, the corresponding values were below 1 mg/L. As the length of the hydrophobic segment increases, the free energy involved in the transference of block copolymer chains from the micelles to the aqueous medium is also larger. It is a consequence of the low chemical affinity between PCL and water and the less favorable entropy contribution for copolymers with greater molecular weight. On the other hand, CMC is less sensitive to the length of PDMAEMA. In each set of copolymers, increasing the length of hydrophilic segment has a minor effect on the CMC value, which is in agreement with other authors [37].

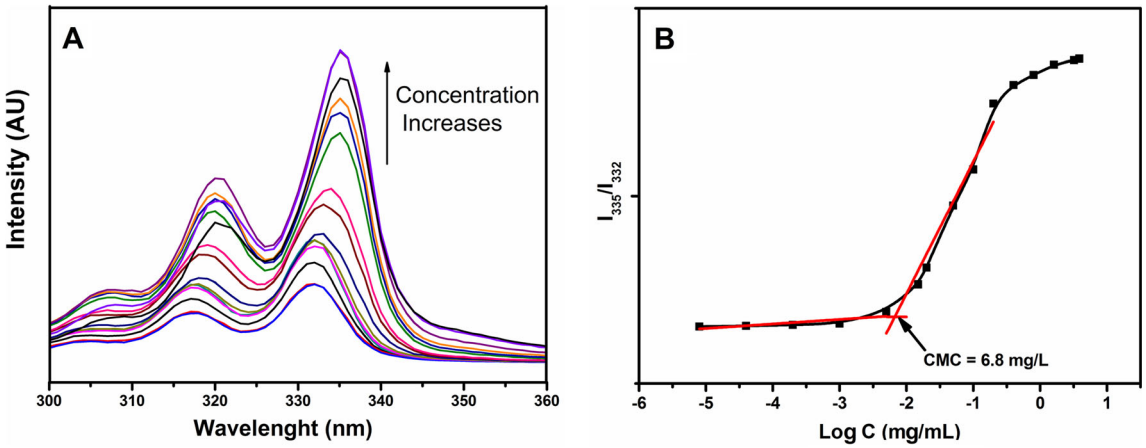

Fig. 4 **a** Steady-state fluorescence excitation spectra monitored at 390 nm for pyrene probe in an aqueous solution of P2D2 in water at pH 5.0 at 25 °C. **b** Plot of I_{335}/I_{332} ratio of pyrene excitation spectra in water as a function of P2D2 triblock copolymer concentration at 25 °C

The most promissory biomedical application of polymer micelles is the encapsulation and solubilization of hydrophobic drugs. The hydrophobicity of the micellar core of aqueous aggregates was estimated measuring the partition equilibrium constant K_v of pyrene, a hydrophobic probe, in the micellar dispersions of PDMAEMA-*b*-PCL-*b*-PDMAEMA copolymers. In this work, K_v was calculated as described by other authors [38, 39]. According to them, pyrene incorporated into the micelles was considered as a simple equilibrium between a micellar phase and a water phase. The ratio of pyrene in the micellar phase to water phase ($[Py]_m/[Py]_w$) can be written as shown in Eq. 5

$$\frac{[Py]_m}{[Py]_w} = \frac{K_v x(c-CMC)}{1000\rho} \quad (5)$$

where x is the weight fraction of the PCL block in the triblock copolymer, c is the concentration of the triblock copolymer, and ρ is the density of PCL core of the micelles, which is assumed to be the bulk density of PCL (1.148 g/cm^3). In the intermediate range of the polymer concentration with substantial increases in the intensity ratios (I_{335}/I_{333}), ($[Py]_m/[Py]_w$) can be written as:

$$\frac{[Py]_m}{[Py]_w} = \frac{(F-F_{min})}{(F_{max}-F)} \quad (6)$$

where F_{min} and F_{max} correspond to the average magnitude of the intensity ratio (I_{335}/I_{332}) in the constant region in the low and high concentration ranges, respectively. F is the intensity ratio (I_{335}/I_{332}) in the intermediate concentration range of the triblock copolymers. Combining Eqs. 5 and 6 yields:

$$\frac{(F-F_{min})}{(F_{max}-F)} = \frac{K_v x(c-CMC)}{1000\rho} \quad (7)$$

K_v values for pyrene listed in Table 2 were obtained by plotting a graph of $(F-F_{min})/(F_{max}-F)$ vs the concentration of the triblock copolymers, as shown in Fig. 5. It is observed that K_v is greater for the largest PCL segment and decreases with

Table 2 Characterization of the micelles obtained by self-assembly of PDMAEMA-*b*-PCL-*b*-PDMAEMA triblock copolymers in aqueous medium at pH 5.0

Sample		DLS Diameter (nm)	ζ (mV) PDI	CMC (mg/L)	$K_v \times 10^5$	pK_a[a]
P2D1 $DMAEMA_{11}$-*b*-CL_{17}-*b*-$DMAEMA_{11}$	57	0.05	22±13	4.9	1.0	7.6±0.3
P2D2 $DMAEMA_{19}$-*b*-CL_{17}-*b*-$DMAEMA_{19}$	82	0.05	25±19	6.8	0.63	7.5±0.2
P2D3 $DMAEMA_{28}$-*b*-CL_{17}-*b*-$DMAEMA_{28}$	85	0.09	27±16	7.4	0.60	7.3±0.2
P10D1 $DMAEMA_{28}$-*b*-CL_{88}-*b*-$DMAEMA_{28}$	46	0.09	41±10	0.86	18	8.3±0.3
P10D2 $MAEMA_{39}$-*b*-CL_{88}-*b*-$DMAEMA_{39}$	47	0.1	30±11	1.0	5.4	8.3±0.4
P10D3 $DMAEMA_{61}$-*b*-CL_{88}-*b*-$DMAEMA_{61}$	54	0.2	37±14	1.0	3.9	7.9±0.2

[a] pK_a were estimated by pH-metric titration of solutions of micelles using a standard solution of HCl 0.021 M. Each value corresponds to the average of three measurements

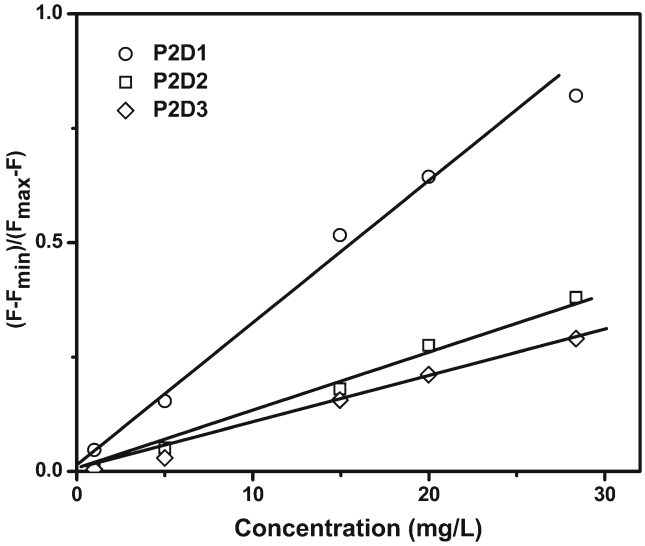

Fig. 5 Plots of $(F-F_{min})/(F_{max}-F)$ vs concentration of P2D1, P2D2, and P2D3 in water

increasing the length of PDMAEMA blocks, suggesting that the micelle core is more hydrophobic for copolymers obtained from PCL of 10 kDa and short PDMAEMA blocks. The values herein reported are close to values early reported for copolymers composed of PCL and PNIPAM [3].

Diameter of the micelles

The diameter and morphology of PMs are parameters that determine their application; for instance, small micelles are suitable for drug delivery applications. These parameters were investigated by DLS and TEM, respectively. The average diameters of the micelles measured at pH 5.0 are listed in Table 2, and Fig. 6a compares the diameter distribution of micelles corresponding to copolymers P2D2 and P10D2. The micelles obtained from each copolymer showed a monomodal distribution centered below 100 nm. It is observed that the diameter of the micelles greatly depends on the PCL length, micelles obtained from the set of copolymers composed of PCL of 10 kDa, are smaller than the corresponding value for copolymer composed of PCL of 2 kDa (see Fig. 6a). On the other hand, as the length of PDMAEMA increases, the diameter of the micelles slightly increases.

The relationship between the diameter of the micelles and the composition of the block copolymers can be explained based on the mechanism for micelle formation. It is that first unimers rapidly associated via nucleation and growth until the micelles have reached a size where further growth increases the free energy of the system [40]. For the set of copolymers obtained from PCL of 10 kDa, the aggregation of the copolymer unimers occurs at lower concentration, as deduced from the lowest CMC, and also present less favorable interactions with water [41], leading to the formation of smaller micelles.

The colloidal stability of the micellar aggregates was determined by measuring its ζ potential; the corresponding values are listed in Table 2. At all the composition, the ζ potential value was larger than +21 mV, which indicates that the micellar dispersions are positively charged and also present colloidal stability. It is observed that the largest PDMAEMA blocks in the copolymer obtained from PCL of 10 kDa, also presents the largest ζ potential.

Figure 6b shows a representative TEM image of micelles obtained from P2D2 copolymer. The image shows spherical micelles dispersed as individual nanoparticles, with diameter in the range between 30 and 100 nm. In the inset, it is observed that the particles are composed by a darker core and a pale shell, which corresponds to the expected morphology of PMs.

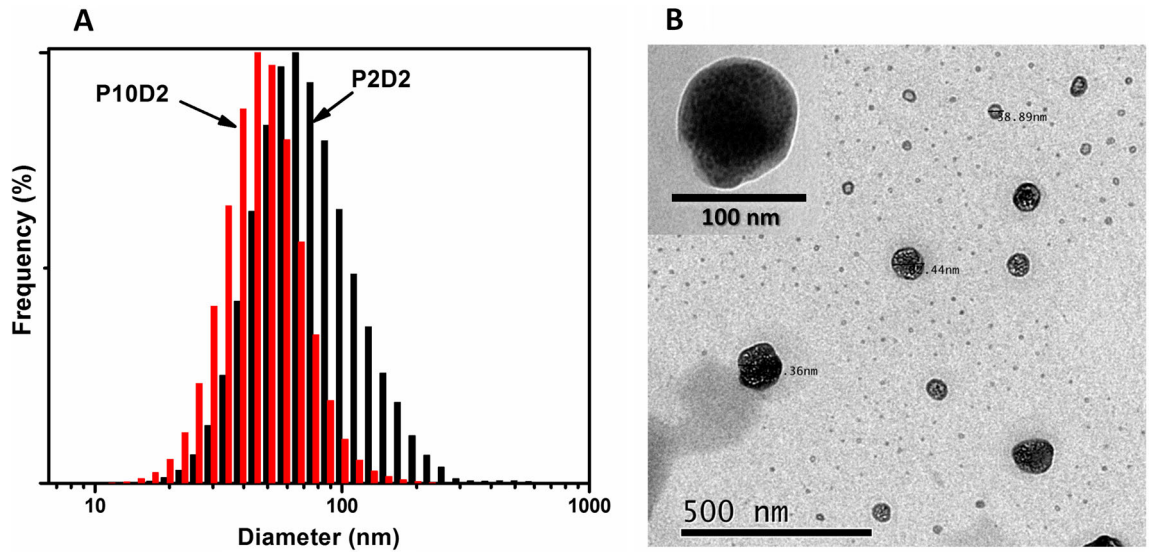

Fig. 6 **a** Particle size distribution of micelles obtained from of P2D2 and P10D2 copolymers. **b** Representative TEM images of micelles obtained by self-assembly of P2D2 in aqueous medium

Table 3 Average diameter and CMC values for representative samples at different pH values

pH	P2D2 DMAEMA$_{19}$-*b*-CL$_{17}$-*b*-DMAEMA$_{19}$ CMC (mg/L)	P10D2 DMAEMA$_{39}$-*b*-CL$_{88}$-*b*-DMAEMA$_{39}$ CMC (mg/L)
5.0	6.8	1.0
6.0	5.2	0.68
7.0	6.1	0.72
7.5	4.2	0.74

Micelles obtained from each copolymer exhibited similar morphology.

Diameters of the particles seen in TEM micrographs are comparable with the values also measure by DLS. However, discrepancy between values determined by both techniques could be attributed to the fact that in the DLS analysis the micelles are hydrated while TEM images are acquired for dried samples [3, 42].

Effect of pH on micelle properties

pK_a values of the copolymers measured by titration (see Table 2) indicate that the segments of PDMAEMA presents a weak basic character, therefore, the properties of the micelles will be affected by the pH of the medium. It is also observed that pK_a slightly depends on the composition of the copolymers, decreases as polymerization degree of DMAEMA increases, which agrees with previous reports [43], and increases for copolymers containing segments of PCL of 10 kDa.

In order to determine the effect of pH on the CMC of PDMAEMA-*b*-PCL-*b*-PDMAEMA copolymers, the CMC values of aqueous dispersions at pH 5.0, 6.0, 7.0, and 7.5 of two representative samples P2D2 and P10D2 were measured by fluorometry (Table 3). It is observed that a pH augment decreases of the CMC; this tendency obeys the protonation degree of the PDMAEMA segment, which in turn is associated to electrostatic repulsion of positively charged DMAEMA units in the hydrophilic blocks [44]. According to Tangeysh et al., the protonation degree is a pH function, thus at pH 5.0 it is higher than 80 %. At pH 6.0, that value is close to 30 % and at pH 7.0 and greater is lower than 10 % [45]. Although the protonation degree notoriously decreases from pH 5.0 to 6.0, the values of CMC present a minor variation. It corroborates that the CMC strongly depends on the length of the hydrophobic segment.

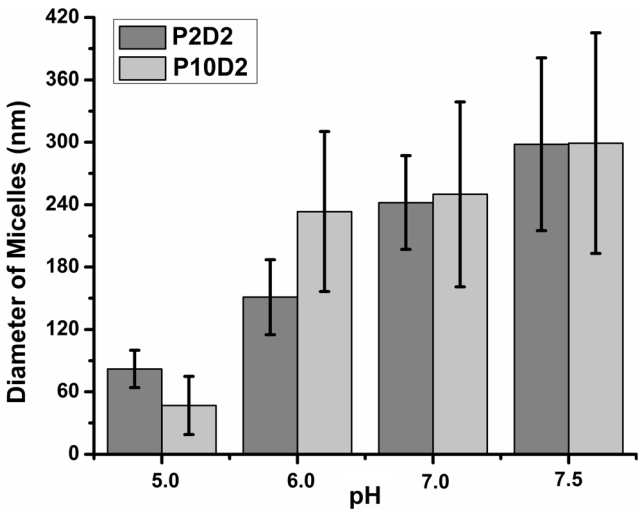

Fig. 7 Particle size of micelles obtained from the self-assembly of P2D2 and P10D2 as a function of pH

The effect of pH on the diameter of micelles obtained from representative samples P2D2 and P10D2 at pH 5.0, 6.0, 7.0, and 7.5 was studied by DLS (Fig. 7). It is observed that as the pH raises, the size of the particles increases. It is presumably due to the aggregation of the particles, facilitated by the lower protonation degree of PDMAEMA and therefore lower interparticle repulsion [18, 20, 44].

Amphotericin B encapsulation

The encapsulation of AmB in micelles obtained by the self-assembly of triblock copolymers PDMAEMA-*b*-PCL-*b*-PDMAEMA with different composition was carried out by partition of AmB in preformed micelles. The loading-efficiency (DLE) as well the AmB content (DLC) determined by Eqs. 1 and 2, respectively, are summarized in Table 4. According to these values, it is deduced that both DLE and DLC depend on the composition of the copolymers. The largest values for these parameters were obtained for micelles formed by copolymer P2D1 that contains the shortest PCL and PDMAEMA segments.

According to the results, a larger and less-dense hydrophobic core favors the encapsulation of AmB. Presumably, the

Table 4 Characterization of the formulations. AmB loading-efficiency and content (n=3)

Sample	Loading-efficiency (%)	AmB content (%)
P2D1 DMAEMA$_{11}$-*b*-CL$_{17}$-*b*-DMAEMA$_{11}$	81.8±5.7	4.1±0.3
P2D2 MAEMA$_{19}$-*b*-CL$_{17}$-*b*-DMAEMA$_{19}$	68.4±4.9	3.4±0.2
P2D3 DMAEMA$_{28}$-*b*-CL$_{17}$-*b*-DMAEMA$_{28}$	57.4±4.7	2.9±0.2
P10D1 (DMAEMA)$_{28}$-*b*-CL$_{88}$-*b*-(DMAEMA)$_{28}$	48.6±2.3	2.4±0.1
P10D2 DMAEMA$_{39}$-*b*-CL$_{88}$-*b*-DMAEMA$_{39}$	46.4±1.5	2.3±0.1
P10D3 DMAEMA$_{61}$-*b*-CL$_{88}$-*b*-DMAEMA$_{61}$	45.2±2.3	2.3±0.1

encapsulation of this substance is limited by the micelle dynamics, which is less favorable for the copolymer containing the largest hydrophobic segment. On the other hand, a shorter hydrophilic shell could reduce the energy barrier require to transfer the AmB from the aqueous medium to the hydrophobic core of the micelles. These results agree with the work previously published by Shim et al. [46].

Conclusions

Amphiphilic triblock copolymers PDMAEMA-*b*-PCL-*b*-PDMAEMA with different composition were successfully synthesized via ATRP. The colloidal properties of micelles obtained via self-assembly of the block copolymers showed to be greatly affected by the length of the hydrophobic segment. The longest hydrophobic block caused the lowest CMC value, smallest particle size, and the most hydrophobic micelle core. The length of the hydrophilic block had a minor effect on the evaluated properties. The encapsulation of AmB showed to depend on micelle dynamics and the length of the hydrophilic segment. Whereas, the hydrophobicity of the micelle core does not seem to be beneficial.

Acknowledgment The authors thank the Pontificia Universidad Javeriana for financial support through grant number 5097.

References

1. Alexandridis P, Lindman B (2000) Amphiphilic block copolymers: self-assembly and applications. Elsevier
2. Torchilin VP (2001) Structure and design of polymeric surfactant-based drug delivery systems. J Control Release 73(2):137–172
3. Loh XJ, Wu YL, Joseph Seow WT, Irzuan Norimzan MN, Zhang Z-X, Xu FJ, Kang ET, Neoh KG, Li J (2008) Micellization and phase transition behavior of thermosensitive poly (*N*-isopropylacrylamide)–poly(ε-caprolactone)–poly(*N*-isopropylacrylamide) triblock copolymers. Polymer 49(23):5084–5094. doi:10.1016/j.polymer.2008.08.061
4. Yoon HJ, Jang WD (2010) Polymeric supramolecular systems for drug delivery. J Mater Chem 20(2):211–222
5. Kore G, Kolate A, Nej A, Misra A (2014) Polymeric micelle as multifunctional pharmaceutical carriers. J Nanosci Nanotechnol 14(1):288–307. doi:10.1166/jnn.2014.9021
6. Sinha V, Bansal K, Kaushik R, Kumria R, Trehan A (2004) Poly-ε-caprolactone microspheres and nanospheres: an overview. Int J Pharm 278(1):1–23
7. Nair LS, Laurencin CT (2007) Biodegradable polymers as biomaterials. Prog Polym Sci 32(8):762–798
8. Gaucher G, Dufresne MH, Sant VP, Kang N, Maysinger D, Leroux JC (2005) Block copolymer micelles: preparation, characterization and application in drug delivery. J Control Release 109(1):169–188
9. Burt HM, Zhang X, Toleikis P, Embree L, Hunter WL (1999) Development of copolymers of poly (D,L-lactide) and methoxypolyethylene glycol as micellar carriers of paclitaxel. Colloids Surf B: Biointerfaces 16(1):161–171
10. Shuai X, Ai H, Nasongkla N, Kim S, Gao J (2004) Micellar carriers based on block copolymers of poly (ε-caprolactone) and poly (ethylene glycol) for doxorubicin delivery. J Control Release 98(3):415–426
11. Aliabadi HM, Elhasi S, Mahmud A, Gulamhusein R, Mahdipoor P, Lavasanifar A (2007) Encapsulation of hydrophobic drugs in polymeric micelles through co-solvent evaporation: the effect of solvent composition on micellar properties and drug loading. Int J Pharm 329(1):158–165
12. Van de Wetering P, Cherng JY, Talsma H, Crommelin DJA, Hennink WE (1998) 2-(Dimethylamino)ethyl methacrylate based (co)polymers as gene transfer agents. J Control Release 53(1–3):145–153. doi:10.1016/S0168-3659(97)00248-4
13. Zhang W, He J, Liu Z, Ni P, Zhu X (2010) Biocompatible and pH-responsive triblock copolymer mPEG-b-PCL-b-PDMAEMA: synthesis, self-assembly, and application. J Polym Sci A Polym Chem 48(5):1079–1091
14. Xu FJ, Li H, Li J, Zhang Z, Kang ET, Neoh KG (2008) Pentablock copolymers of poly(ethylene glycol), poly((2-dimethyl amino)ethyl methacrylate) and poly(2-hydroxyethyl methacrylate) from consecutive atom transfer radical polymerizations for non-viral gene delivery. Biomaterials 29(20):3023–3033. doi:10.1016/j.biomaterials.2008.03.041
15. Zhu C, Jung S, Luo S, Meng F, Zhu X, Park TG, Zhong Z (2010) Co-delivery of siRNA and paclitaxel into cancer cells by biodegradable cationic micelles based on PDMAEMA–PCL–PDMAEMA triblock copolymers. Biomaterials 31(8):2408–2416
16. Xu F, Neoh K, Kang E (2009) Bioactive surfaces and biomaterials via atom transfer radical polymerization. Prog Polym Sci 34(8):719–761
17. Qian X, Long L, Shi Z, Liu C, Qiu M, Sheng J, Pu P, Yuan X, Ren Y, Kang C (2014) Star-branched amphiphilic PLA-b-PDMAEMA copolymers for co-delivery of miR-21 inhibitor and doxorubicin to treat glioma. Biomaterials 35(7):2322–2335. doi:10.1016/j.biomaterials.2013.11.039
18. Lee AS, Gast AP, Bütün V, Armes SP (1999) Characterizing the structure of pH dependent polyelectrolyte block copolymer micelles. Macromolecules 32(13):4302–4310
19. Baines F, Billingham N, Armes S (1996) Synthesis and solution properties of water-soluble hydrophilic-hydrophobic block copolymers. Macromolecules 29(10):3416–3420
20. Liu S, Weaver JV, Tang Y, Billingham NC, Armes SP, Tribe K (2002) Synthesis of shell cross-linked micelles with pH-responsive cores using ABC triblock copolymers. Macromolecules 35(16):6121–6131
21. Matyjaszewski K, Tsarevsky NV (2014) Macromolecular engineering by atom transfer radical polymerization. J Am Chem Soc 136(18):6513–6533. doi:10.1021/ja408069v
22. Ran J, Wu L, Zhang Z, Xu T (2014) Atom transfer radical polymerization (ATRP): a versatile and forceful tool for functional membranes. Prog Polym Sci 39(1):124–144. doi:10.1016/j.progpolymsci.2013.09.001
23. Guo S, Qiao Y, Wang W, He H, Deng L, Xing J, Xu J, Liang XJ, Dong A (2010) Polycaprolactone-graft-poly(2-(*N*,*N*-dimethylamino) ethyl methacrylate) nanoparticles: pH dependent thermo-sensitive multifunctional carriers for gene and drug delivery. J Mater Chem 20(33):6935–6941. doi:10.1039/C0JM00506A
24. Lin D, Jiang Q, Cheng Q, Huang Y, Huang P, Han S, Guo S, Liang Z, Dong A (2013) Polycation-detachable nanoparticles self-assembled from mPEG-PCL-g-SS-PDMAEMA for in vitro and *in vivo* siRNA delivery. Acta Biomater 9(8):7746–7757. doi:10.1016/j.actbio.2013.04.031
25. Yue X, Qiao Y, Qiao N, Guo S, Xing J, Deng L, Xu J, Dong A (2010) Amphiphilic methoxy poly (ethylene glycol)-b-poly(ε-caprolactone)-b-poly(2-dimethylaminoethyl methacrylate) cationic copolymer nanoparticles as a vector for gene and drug delivery. Biomacromolecules 11(9):2306–2312. doi:10.1021/bm100410m
26. Zhang Y, He J, Cao D, Zhang M, Ni P (2014) Galactosylated reduction and pH dual-responsive triblock terpolymer Gal-PEEP-a-

PCL-ss-PDMAEMA: a multifunctional carrier for the targeted and simultaneous delivery of doxorubicin and DNA. Polym Chem 5(17): 5124–5138. doi:10.1039/C4PY00538D
27. Han S, Wan H, Lin D, Guo S, Dong H, Zhang J, Deng L, Liu R, Tang H, Dong A (2014) Contribution of hydrophobic/hydrophilic modification on cationic chains of poly(ε-caprolactone)-graft-poly(dimethylamino ethylmethacrylate) amphiphilic co-polymer in gene delivery. Acta Biomater 10(2):670–679. doi:10.1016/j.actbio.2013.09.035
28. Lo YL, Chen GJ, Feng TH, Li MH, Wang LF (2014) Synthesis and characterization of S-PCL-PDMAEMA for co-delivery of pDNA and DOX. RSC Adv 4(22):11089–11098. doi:10.1039/C3RA46914J
29. Deray G (2002) Amphotericin B nephrotoxicity. J Antimicrob Chemother 49(suppl 1):37–41
30. Rao JP, Geckeler KE (2011) Polymer nanoparticles: preparation techniques and size-control parameters. Prog Polym Sci 36(7):887–913
31. Maiti S, Chatterji PR, Nisha C, Manorama S, Aswal VK, Goyal PS (2001) Aggregation and polymerization of PEG-based macromonomers with methacryloyl group as the only hydrophobic segment. J Colloid Interface Sci 240(2):630–635
32. Shim WS, Kim SW, Choi EK, Park HJ, Kim JS, Lee DS (2006) Novel pH sensitive block copolymer micelles for solvent free drug loading. Macromol Biosci 6(2):179–186
33. Motala-Timol S, Jhurry D (2007) Synthesis of PDMAEMA–PCL–PDMAEMA triblock copolymers. Eur Polym J 43(7):3042–3049
34. San Miguel V, Limer A, Haddleton DM, Catalina F, Peinado C (2008) Biodegradable and thermoresponsive micelles of triblock copolymers based on 2-(*N*,*N*-dimethylamino) ethyl methacrylate and ε-caprolactone for controlled drug delivery. Eur Polym J 44(11):3853–3863
35. Mok MM, Thiagarajan R, Flores M, Morse DC, Lodge TP (2012) Apparent critical micelle concentrations in block copolymer/ionic liquid solutions: remarkably weak dependence on solvophobic block molecular weight. Macromolecules 45(11):4818–4829
36. Li X, Mya KY, Ni X, He C, Leong KW, Li J (2006) Dynamic and static light scattering studies on self-aggregation behavior of biodegradable amphiphilic poly (ethylene oxide)-poly [(R)-3-hydroxybutyrate]-poly (ethylene oxide) triblock copolymers in aqueous solution. J Phys Chem B 110(12):5920–5926
37. Gohy JF (2005) Block copolymer micelles. In: Abetz V (ed) Block copolymers II, vol 190. Advances in polymer science. Springer, Berlin, pp 65–136. doi:10.1007/12_048
38. Wilhelm M, Zhao CL, Wang Y, Xu R, Winnik MA, Mura JL, Riess G, Croucher MD (1991) Poly (styrene-ethylene oxide) block copolymer micelle formation in water: a fluorescence probe study. Macromolecules 24(5):1033–1040. doi:10.1021/ma00005a010
39. Allcock HR, Cho SY, Steely LB (2006) New amphiphilic poly [bis(2,2,2-trifluoroethoxy)phosphazene]/poly(propylene glycol) triblock copolymers: synthesis and micellar characteristics. Macromolecules 39(24):8334–8338. doi:10.1021/ma061531w
40. Nicolai T, Colombani O, Chassenieux C (2010) Dynamic polymeric micelles versus frozen nanoparticles formed by block copolymers. Soft Matter 6(14):3111–3118. doi:10.1039/B925666K
41. Zamfir M, Patrickios CS, Montagne F, Abetz C, Abetz V, Oss-Ronen L, Talmon Y (2012) Styrene-vinyl pyridine diblock copolymers: synthesis by RAFT polymerization and self-assembly in solution and in the bulk. J Polym Sci A Polym Chem 50(8):1636–1644
42. Zhang X, Zhu X, Ke F, Ye L, EQ C, AY Z, ZG F (2009) Preparation and self-assembly of amphiphilic triblock copolymers with polyrotaxane as a middle block and their application as carrier for the controlled release of amphotericin B. Polymer 50(18):4343–4351
43. van de Wetering P, Zuidam NJ, van Steenbergen MJ, van der Houwen OAGJ, Underberg WJM, Hennink WE (1998) A mechanistic study of the hydrolytic stability of poly(2-(dimethylamino)ethyl methacrylate). Macromolecules 31(23):8063–8068. doi:10.1021/ma980689g
44. Chen WY, Alexandridis P, Su CK, Patrickios CS, Hertler WR, Hatton TA (1995) Effect of block size and sequence on the micellization of ABC triblock methacrylic polyampholytes. Macromolecules 28(25): 8604–8611. doi:10.1021/ma00129a020
45. Tangeysh B, Fryd M, Ilies MA, Wayland BB (2012) Palladium metal nanoparticle size control through ion paired structures of [PdCl4]2– with protonated PDMAEMA. Chem Commun 48(71):8955–8957. doi:10.1039/C2CC34401G
46. Shim YH, Lee HJ, Dubois P, Chung CW, Jeong YI (2011) Amphotericin B aggregation inhibition with novel nanoparticles prepared with poly(ε-caprolactone)/poly(*N*,*N*-dimethylamino-2-ethyl methacrylate) diblock copolymer. J Microbiol Biotechnol 21(1):28–36